PLISKA
STUDIA MATHEMATICA BULGARICA

ПЛИСКА
БЪЛГАРСКИ МАТЕМАТИЧЕСКИ СТУДИИ

Pliska Stud. Math. Bulgar. **23** (2014), 175–188

PLISKA
STUDIA MATHEMATICA
BULGARICA

2D FRACTURE PROBLEMS IN MAGNETO-ELECTRO-ELASTIC COMPOSITE MATERIALS UNDER ANTI-PLANE WAVES BY BIEM

Yonko Stoynov

Abstract. Magneto-electro-elastic material with two cracks is studied. The material is subjected to harmonic anti-plane mechanical and in-plane electric and magnetic load. The boundary value problem for the coupled system of partial differential equations is solved numerically by the Boundary integral equation method (BIEM). Program code in FORTRAN 77 based on the BIEM is developed. The numerical solution is compared with the results obtained by the dual integral equations method. Numerical simulations show the dependence of the stress, electric and magnetic field concentration near the crack tips on the normalized frequency of the applied dynamic load for different locations and dispositions of the cracks.

1. Introduction

In recent years a great attention has been paid to magneto-electro-elastic materials (MEEM). These materials are used extensively in modern electronic industry, because of their ability to convert mechanical energy into electrical and magnetic and vice versa. They possess magnetoelectric (ME) property observed for the first time by Astrov in 1960 in the single-phased material Cr_2O_3. Single-phased magnetoelectric materials have two main drawbacks - ME effect takes place at low temperatures and the effect is very weak. ME property in magnetoelectroelastic composite materials is reported for the first time by Van Suchtelen [1] in

2000 *Mathematics Subject Classification:* Math.Subj. Class.
Key words: key words

1972. Unlike single-phased materials they possess large ME effect at ambient temperatures, which makes them suitable for applications. Owing to this, these composites are potential candidates for fabricating a new generation of smart or intelligent structures.

An important feature of MEEM is their brittleness. Cracks inevitably exist in these materials. When subjected to external load the cracks may extend and as a result the material may lose its structural integrity and/or functional properties. To understand the failure mechanism of such materials fracture mechanics analysis is prerequisite.

In this study we will consider MEEM with more than one crack subjected to SH waves. Numerical results are obtained using the BIEM and show the dependance of the stress intensity factors on: (a) the frequency of the applied external load; (b) the wave propagation direction; (c) the type of the dynamic load; (d) the number of cracks and their geometrical configuration; (e) the direction and magnitude of the material gradient; (f) the crack interaction.

2. Statement of the problem

We consider transversely-isotropic functionally graded magnetoelectroelastic material in the coordinate system $Ox_1x_2x_3$, where Ox_3 is the poling direction and symmetry axis and Ox_1x_2 is the isotropic plane. MEEM is subjected to anti-plane mechanical impact on the Ox_3 axis, and in-plane electrical and magnetic impacts in the plane Ox_1x_2. The geometry of this problem is given in Figure 1, where Cr_1 and Cr_2 denote the section of the plane Ox_1x_2 with the two cracks. The constitutive equations for this type of medium (see Soh and Liu [2]) are:

$$\sigma_{iQ} = C_{iQJl}u_{J,l}. \tag{1}$$

Here and in what follows comma denotes partial differentiation, it is assumed summation in repeating indexes and small indexes vary $1, 2$, while capital indexes vary $3, 4, 5$; u_J is the generalized displacement vector $u_J = (u_3, \phi, \varphi)$, where u_3 is the elastic displacement, ϕ is the electric potential, φ is the magnetic potential; $\sigma_{iJ} = (\sigma_{i3}, D_i, B_i)$ is the generalized stress tensor, where σ_{iJ} is the stress, D_i and B_i are the components of the electric and magnetic induction respectively along Ox_i axis; C_{iQJl} is the generalized elasticity tensor defined as: $C_{i33l}(x) = \begin{cases} c_{44}(x), i = l \\ 0, \quad i \neq l \end{cases}$, $C_{i34l}(x) = C_{i43l}(x) = \begin{cases} e_{15}(x), i = l \\ 0, \quad i \neq l \end{cases}$, $C_{i35l}(x) = C_{i53l}(x) = \begin{cases} q_{15}(x), i = l \\ 0, \quad i \neq l \end{cases}$, $C_{i44l}(x) = \begin{cases} -\varepsilon_{11}(x), i = l \\ 0, \qquad i \neq l \end{cases}$, $C_{i45l}(x) =$

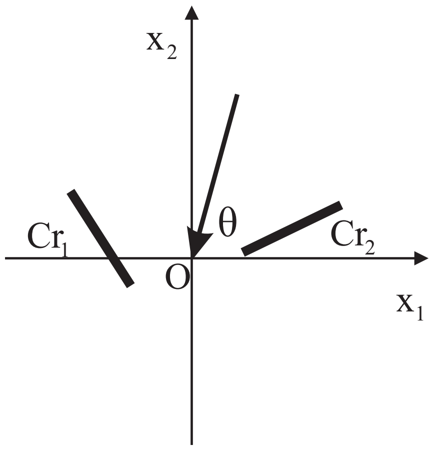

Figure 1 – Two cracks in a magnetoelectroelastic plane, θ is the incident wave angle

$C_{i54l}(x) = \begin{cases} -d_{11}(x), i = l \\ 0, \quad\quad i \neq l \end{cases}$, $C_{i55l}(x) = \begin{cases} -\mu_{11}(x), i = l \\ 0, \quad\quad i \neq l \end{cases}$, where $x = (x_1, x_2)$. Functions $c_{44}(x)$, $e_{15}(x)$, $\varepsilon_{11}(x)$ are: elastic stiffness, piezoelectric coupled coefficient and dielectric permittivity, while $q_{15}(x)$, $d_{11}(x)$, $\mu_{11}(x)$ are piezomagnetic, magnetoelectric coefficients and magnetic permeability correspondingly.

Assuming electric and magnetic fields as static the governing equation in the frequency domain in absence of body force, electric charge and magnetic current can be written as follows:

$$\sigma_{iQ,i} + \rho_{QJ}\omega^2 u_J = 0, \tag{2}$$

where $\rho_{QJ} = \begin{cases} \rho, Q = J = 3 \\ 0, Q, J = 4 \text{ or } 5 \end{cases}$, $\rho(x)$ is the mass density, $\omega > 0$ is the frequency.

We assume that all material properties depend on x in one and the same way and describe this by an inhomogeneity function $g(x)$: $c_{44}(x) = g(x)c_{44}$, $e_{15}(x) = g(x)e_{15}$, $\varepsilon_{11}(x) = g(x)\varepsilon_{11}$, $q_{15}(x) = g(x)q_{15}$, $d_{11}(x) = g(x)d_{11}$, $\mu_{11}(x) = g(x)\mu_{11}$. The inhomogeneity function has the following form: $g(x) = e^{2\langle k,x\rangle}$, where $\langle k, x\rangle = k_1x_1 + k_2x_2$.

When the incident SH wave interacts with the cracks a scattered wave is produced. The total displacement and traction at any point of the plane can be calculated by the superposition principle:

$$u_J = u_J^{in} + u_J^{sc}, t_J = t_J^{in} + t_J^{sc}, \tag{3}$$

where $t_J = \sigma_{iJ} n_i$, $n_i = (n_1, n_2)$ is the outer normal vector, u_J^{in} and t_J^{in} are the displacement and traction of the incident wave fields respectively, u_J^{sc} and t_J^{sc} are the scattered by the cracks wave fields. We impose the following boundary conditions:

$$t_J = 0 \ \ or \ \ t_J^{in} = -t_J^{sc}, \quad x \in Cr = Cr_1 \bigcup Cr_2, \tag{4}$$

$$u_J^{sc} \to 0 \ \ when \ \ (x_1^2 + x_2^2)^{1/2} \to \infty. \tag{5}$$

The boundary condition (4) means that the cracks are free of mechanical traction and also they are magnetoelectrically impermeable. This boundary condition is widely used in literature, see Sladek et al. [3]. Boundary conditions for permeable cracks are also studied. Impermeable and permeable crack models are discussed in details in Dineva et al. [4]. The boundary value problem (2), (4) and (5) is reduced to an equivalent system of integro-differential equations along the cracks and then solved numerically.

3. Boundary integral equation method

The fundamental solution u_{KM}^* of (2) can be represented in the following way:

$u_{KM}^* = e^{-<k,x>} U_{KM}^*$,

where U_{KM}^* is the solution of:

$C_{iJKi} U_{KM,ii}^* + [\rho_{JK}\omega^2 - C_{iJKi} k_i^2] U_{KM}^* = e^{-<k,x>}(\xi)\delta_{JM}\delta(x,\xi)$.

In this equation δ_{JM} is the Kronecker's symbol and $\delta(x,\xi)$ is the Dirak delta function. We define: $\omega_0 = \sqrt{\frac{\det M}{(\varepsilon_{11}\mu_{11} - d_{11}^2 \rho)}} |k|$, where $M = \begin{pmatrix} c_{44} & e_{15} & q_{15} \\ e_{15} & -\varepsilon_{11} & -d_{11} \\ q_{15} & -d_{11} & -\mu_{11} \end{pmatrix}$, $|k| = \sqrt{k_1^2 + k_2^2}$.

Three cases with respect to ω are possible:

(i) $\omega > \omega_0$ – wave propagation;

(ii) $\omega = \omega_0$ – "static" behavior, a critical frequency;

(iii) $\omega < \omega_0$ – simple vibration.

We will consider the first case in which we have wave propagation.

Following Wang and Zhang [5] and Gross et al. [6] the following representation formulae are valid:

$$
\begin{aligned}
(6)\qquad & t^{sc}_J(x,\omega) = C_{iJKl}(x)n_i(x)\int_{Cr}\{[\sigma^*_{\eta PK}(x,y,\omega)\triangle u_{P,\eta}(y,\omega)\\
& -\rho_{QP}(y)\omega^2 u^*_{QK}(x,y,\omega)\triangle u_P(y)]\delta_{\lambda l}\\
& -\sigma^*_{\lambda PK}(x,y,\omega)\triangle u_{P,l}(y,\omega)]n_\lambda(y)\}d\Gamma(y),
\end{aligned}
$$

$$
(7)\qquad u^{sc}_J(x,\omega) = \int_{Cr}\sigma^*_{\eta MJ}(x,y,\omega)\triangle u_M(y,\omega)n_\eta(y)d\Gamma,
$$

where $\Delta u_J = u_J|_{Cr^+} - u_J|_{Cr^-}$ are jumps of the displacement along the cracks or crack opening displacement (COD), $Cr = Cr_1\bigcup Cr_2$, Cr^+ and Cr^- are the upper and lower bounds of the cracks correspondingly, u^*_{KM} is the fundamental solution and $\sigma^*_{iJK} = C_{iJMl}u^*_{KM,l}$. Boundary condition (5) is satisfied because of (7) and the limit $\sigma^*_{\eta MJ}(x,y,\omega)\to 0$, when $x\to\infty$. Since the fundamental solution and the incident wave field are known, using (6) we obtain an integro-differential equation along the crack, where unknowns are COD:

$$
\begin{aligned}
(8)\qquad & t^{in}_J(x,\omega) = -C_{iJKl}(x)n_i(x)\int_{Cr}\{[\sigma^*_{\eta PK}(x,y,\omega)\triangle u_{P,\eta}(y,\omega)\\
& -\rho_{QP}(y)\omega^2 u^*_{QK}(x,y,\omega)\triangle u_P(y)]\delta_{\lambda l}\\
& -\sigma^*_{\lambda PK}(x,y,\omega)\triangle u_{P,l}(y,\omega)]n_\lambda(y)\}d\Gamma(y), x\in Cr.
\end{aligned}
$$

The equation (8) is solved numerically. Once COD are found we can calculate the scattered field at every point on the plane using (6).

4. Numerical realization and results

The two cracks are discretisized using 7BE for each crack. The unknown COD are approximated by parabolic shape functions. The singular integrals are solved analytically using asymptotic behavior of the fundamental solution for small arguments. The 2D integrals are solved numerically by the Monte-Carlo method. Program code in FORTRAN 77 is developed.

The generalized stress intensity factors are computed as follows:
Stress intensity factor(SIF): $K_{III} = \lim_{x_1\to\pm a} t_3\sqrt{2\pi(x_1\mp a)}$,
Electric field intensity factor(EFIF): $K_E = \lim_{x_1\to\pm a} E_2\sqrt{2\pi(x_1\mp a)}$,
Magnetic field intensity factor(MFIF): $K_H = \lim_{x_1\to\pm a} H_2\sqrt{2\pi(x_1\mp a)}$.

The half-length of the cracks is $a = 5mm$. The MEEM used in this study is the piezoelectric/piezomagnetic composite $BaTiO_3/CoFe_2O_4$. The material constants for this composite can be found in Song and Sih [7], Li [8]. The components of the inhomogeneity function are presented in the following way: $k = (k_1,k_2) = \frac{\beta}{2a}(\cos\alpha,\sin\alpha)$, where β is the magnitude of inhomogeneity, α is the inhomogeneity angle.

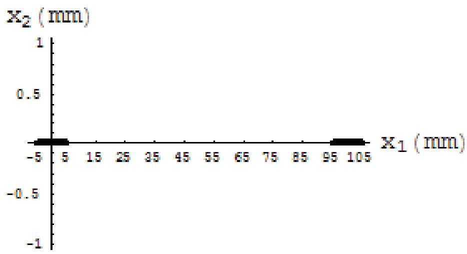

Figure 2 – Two collinear cracks in a magnetoelectroelastic plane

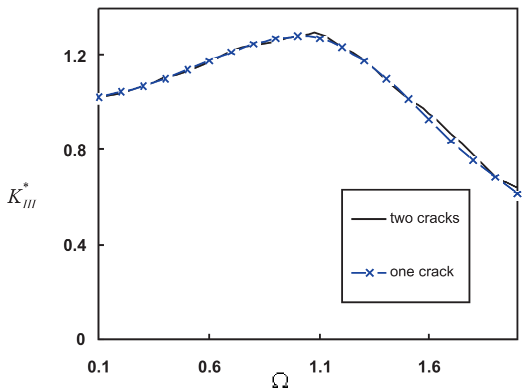

Figure 3 – The normalized SIF versus the normalized frequency for two collinear cracks when the distance between them is very large

4.1. Validation

The proposed numerical scheme is validated using the solution for one crack and solutions obtained by the dual integral equation method. In the first example we consider two collinear cracks when the distance between them is very large (see Figure 2). Since the crack interaction is minimal in this case, we expect the result to converge to the result for one crack. The comparison is given in Figure 3. The difference is no more than 4 % for large frequencies. The normalized SIF is $K^*_{III} = \frac{K_{III}}{t_3^{in}\sqrt{(\pi a)}}$ and the normalized frequency is $\Omega = a\omega\sqrt{(\rho c_{44}^{-1})}$.

As another example we consider two parallel cracks (see Figure 4) at a large distance from one another. The difference between the results for one and two parallel cracks is no more than 4% (see Figure 5).

The comparison with the results of Zhou and Wang [9] obtained by the dual integral equation method is given in Figures 6 and 7. The results for the normalized

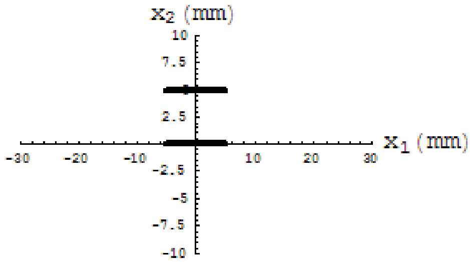

Figure 4 – Two parallel cracks in a magnetoelectroelastic plane

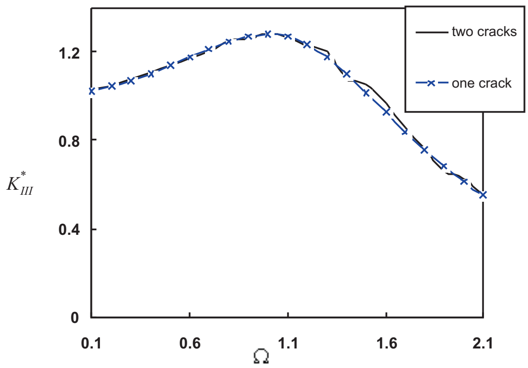

Figure 5 – The normalized SIF versus the normalized frequency for two parallel cracks at a large distance from one another

SIF versus h/a for static external load are shown in Figure 6. Here and in what follows h is the distance between the cracks. In this example $h = 0.1a, 0.5a, a, ..., 6a$. Results for the same scenario, but for dynamic load ($\Omega = 0.4$) are given in Figure 7. In both case the difference is no more 1.5-2%.

4.2. Parametric studies

In parametric studies we show the sensitivity of the generalized SIF to the distance between the cracks, the angle of the incident wave, the cracks disposition and the angle and the magnitude of the inhomogeneity gradient.

Results for normalized SIF, EFIF and MFIF versus the normalized frequency for collinear cracks are presented in figures 8 a),b) and c). The normalized EFIF and MFIF are respectively $K_E^* = 10\frac{K_E}{t_3^{in}\sqrt{(\pi a)}}$ and $K_H^* = 10^4\frac{K_H}{t_3^{in}\sqrt{(\pi a)}}$. The material is homogeneous, the incident wave is normal and distance between the cracks is

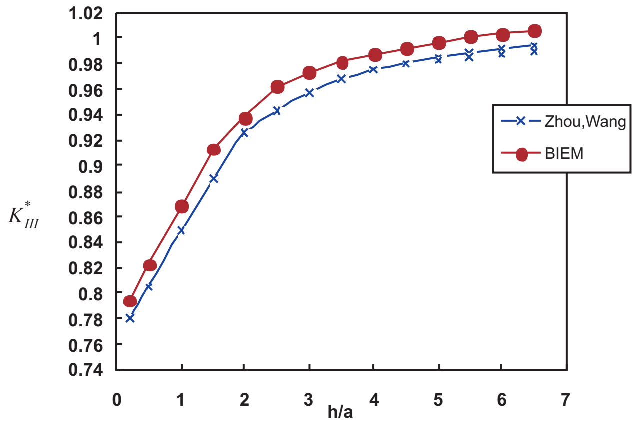

Figure 6 – The normalized SIF versus the distance between the cracks, static case

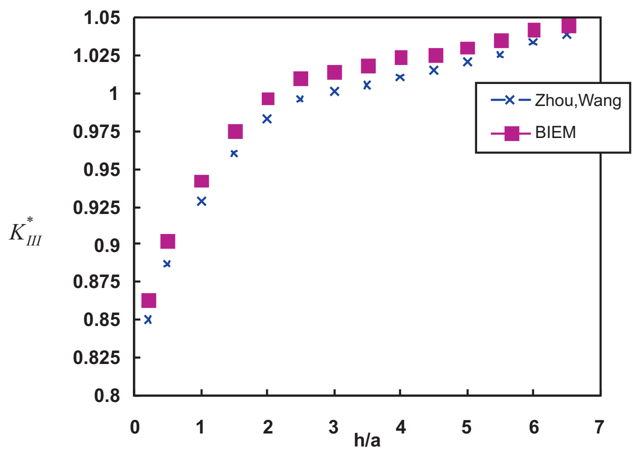

Figure 7 – The normalized SIF versus the distance between the cracks, dynamic case

changing: $h = 0.25a, 0.5a, a, 2a$. We see increasing of the generalized SIF, when the distance is decreasing.

In Figure 9 we present results for collinear cracks, when the distance between them is fixed $h = 2.5mm$. The material is homogeneous. The incident wave angle is changing: $\theta = 15°, 30°, ..., 90°$. For large frequencies the presented results show increasing of SIF, when the angle θ is decreasing. The opposite is true for smaller frequencies. The numerical values are calculated at the right crack tip of the left crack.

Results for parallel cracks are given in Figures 10 a), b) and c). In Figures 10 a) and b) the distance between the cracks is increasing $h = 6, 9, 12mm$ and incident wave angle is $\pi/2$ and $\pi/3$ respectively. The material is homogeneous. We observe increasing of the SIF when the distance is increasing. This is the crack shielding effect discussed in Ratwanni [10]. In Figures 10 c) the distance between the cracks is fixed $h = 3mm$ and the incident wave angle θ is changing: $\theta = \pi/6, \pi/3, \pi/2$. The results show increasing of the SIF at the right crack tip with decreasing of the angle of the incident wave.

The dependance of the generalized SIF on the normalized frequency for inhomogeneous materials is presented in Figures 11 a), b) and c). The cracks are collinear and the distance between them is fixed $h = 2.5mm$. The inhomogeneity angle is $\alpha = \pi/2$, the inhomogeneity magnitude β is changing. The results show increasing of SIF, EFIF and MFIF with increasing of the magnitude near the critical frequencies. The opposite is the case for the larger frequencies: SIF, EFIF and MFIF are decreasing with increasing of the magnitude.

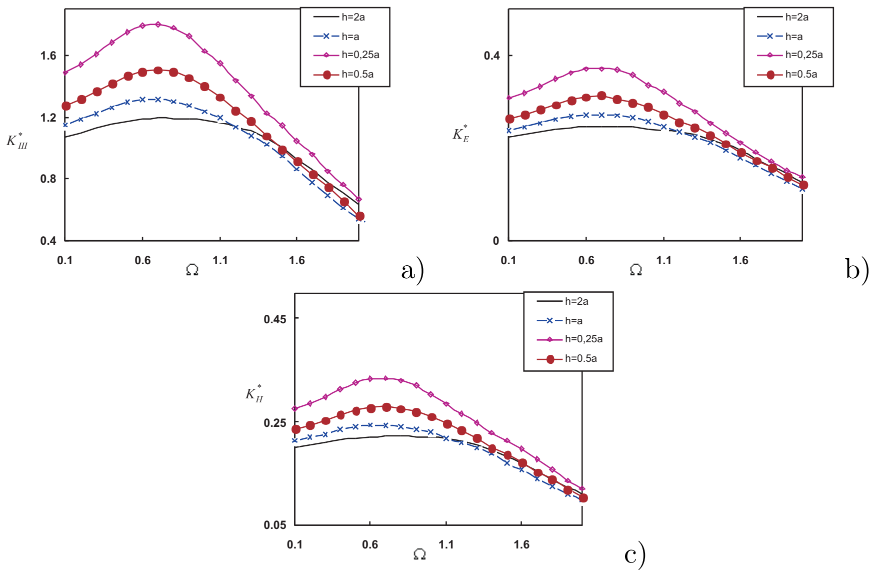

Figure 8 – The generalized SIF versus the normalized frequency in a homogeneous magnetoelectroelastic plane subjected to an incident SH wave: (a) K^*_{III} ; (b) K^*_E; (c) K^*_H.

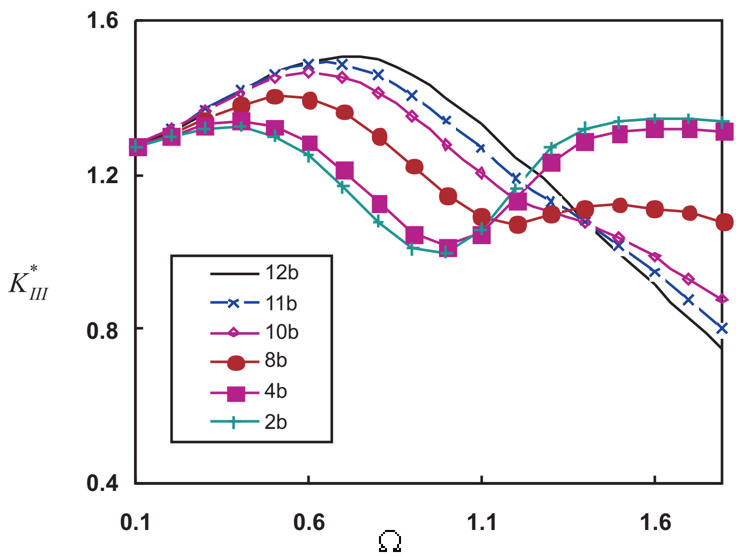

Figure 9 – The normalized SIF versus the normalized frequency when the incident wave angle θ varies, $b = 7.5°$

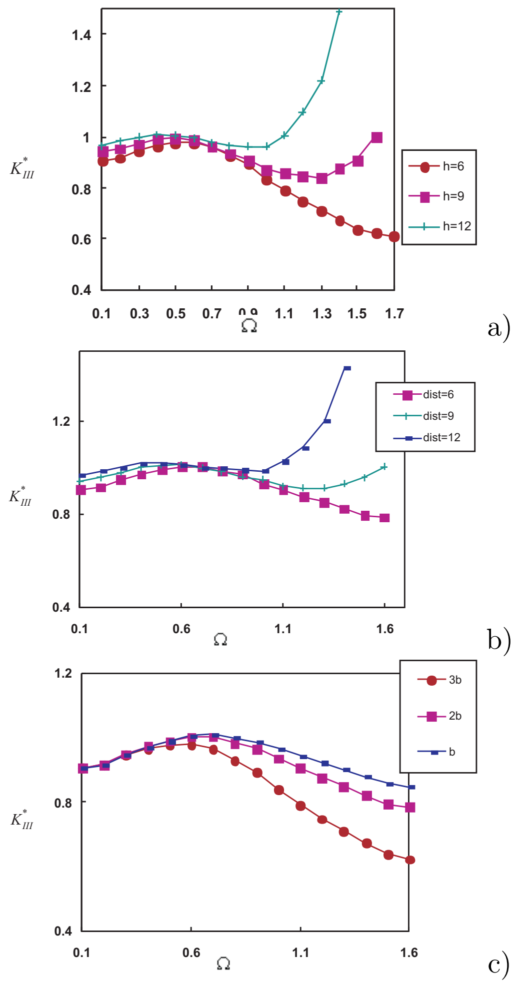

Figure 10 – The normalized SIF versus the normalized frequency for parallel cracks: (a) the incident wave angle is $\pi/2$; (b) the incident wave angle is $\pi/3$; (c) the incident wave angle θ varies, $b = \pi/6$.

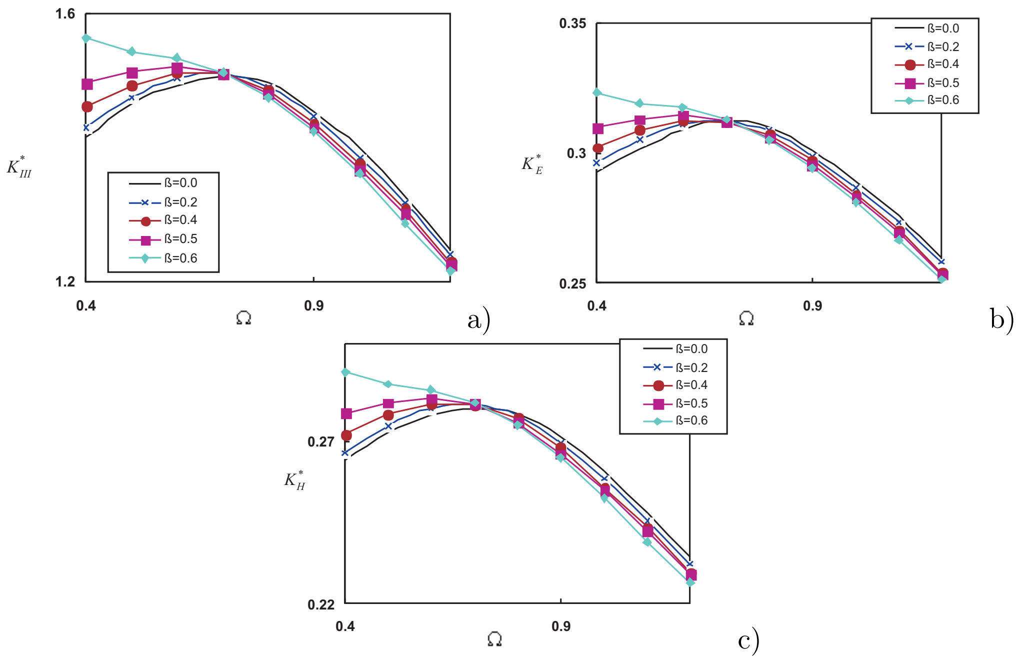

Figure 11 – The generalized SIF versus the normalized frequency for inhomogeneous material, the inhomogeneity angle $\alpha = \pi/2$, the inhomogeneity magnitude β is increasing: (a)K^*_{III} ; (b) K^*_E; (c) K^*_H.

5. Conclusion

In this paper we study MEEM with two cracks, subjected to antiplane mechanical and inplane electrical and magnetic external load by BIEM. FORTRAN 77 software is developed for the numerical solution. The sensitivity of the generalized SIF to the distance between cracks, the cracks disposition, the incident wave angle, the inhomogeneity magnitude and angle and the crack interaction is shown. For parallel cracks crack shielding effect is observed. The obtained results can be applied for developing new non-destructive test methods for monitoring integrity and reliability of modern smart materials and structures.

References

[1] Van Suchtelen, *Product properties: a new application of composite materials*, Phillips Research Reports, **27**, (1972), 28–37

[2] A. K. Soh, J. X. Liu, *On the constitutive equations of magnetoelectroelastic solids*, J. Intell. Mater. Syst. Struct., **16**, (2005), 597–602 J. Intell. Mater. Syst. Struct.

[3] J. Sladek, V. Sladek, P. Solek, E. Pan, *Fracture analysis of cracks in magneto-electro-elastic solids by the MLPG*, Comput Mech, **42**, (2008), 697–714

[4] P. Dineva, D. Gross, R. Müller, Ts. Rangelov, *Dynamic Fracture of Piezoelectric Materials*, Series: Solid Mechanics and Its Applications, **212**, Springer (2014)

[5] C.-Y. Wang and C. Zhang, *2D and 3D dynamic Green's functions and time domain BIE formulations for piezoelectric solids*, Proceedings of the WCCM VI in conjunction with APCOM'04 September 5-10, Z. H. Yao, M. W. Yuan, W. X. Zhong, (Eds.), Tsingua University Press and Springer-Verlag, Beijing, China (2004)

[6] D. Gross, T. Rangelov, P. Dineva, *2D Wave Scattering by a Crack in a Piezoelectric Plane Using Traction BIEM*, Journal Structural Integrity and Durability, **1**, Tech Science Press (2005), 35–47

[7] Z. F. Song, G. C. Sih, *Crack Initiation Behaviour in Magneto-Electro-Elastic Composite Under In-Plane Deformation*, Theor. Appl. Fract. Mech., **39**, (2003), 189–207

[8] X. F. Li, *Dynamic analysis of a cracked magnetoelectroelastic medium under antiplane mechanical and inplane electric and magnetic impacts*, Int. J. Solids and Str., **42**, (2005), 3185–3205

[9] Z. Zhou, B. Wang, *Dynamic behavior of two parallel symmetry cracks in magneto-electro-elastic composites under harmonic anti-plane waves*, Applied Mathematics and Mechanics (English Edition), **27**, (2006), 583–591

[10] M. Ratwani, G D. Gupta, *Interaction between parallel cracks in layered composites*, Intern. Journal of Solids and Structures, **10**, (1974), 701–708

Yonko Stoynov
Technical University of Sofia, Bulgaria
*e-mail:*jds@tu-sofia.bg